ITERATIVE MULTI-USER DECODING FOR MIMO-OFDM SYSTEMS OVER TIME-FREQUENCY VARIANT WIRELESS CHANNELS

Pierluigi Salvo Rossi

Dept. of Electronics and Telecommunications, *Norwegian Univ. of Science and Technology*,
O.S. Bragstads plass 2B, 7491 Trondheim, Norway, email:salvoros@iet.ntnu.no}

ABSTRACT

An iterative receiver for Multiple-Input Multiple-Output (MIMO) Orthogonal Frequency Division Multiplexing (OFDM) systems in time-frequency wireless channels is presented. Multi-User Detection (MUD) and Channel Estimation (CE) are performed using soft information iteratively provided by the single-user decoders. Bidimensional Slepian expansion exploits time and frequency channel variation. Performance of the system are presented via numerical simulations.

1. INTRODUCTION

Future wireless communications will combine different advanced techniques such as multiple antennas and multi-carrier modulation to provide high data rates [1]. Multiple-Input Multiple-Output (MIMO) systems increase capacity proportionally to the minimum number of transmit and receive antennas while Orthogonal Frequency Division Multiplexing (OFDM) simplifies channel equalization at receiver side. Iterative receivers for Multi-User Detection (MUD) [2, 3, 4] achieve near-optimum performance with contained complexity. Recent architectures [5, 6, 7] perform in the iterative loop MUD, single-user decoding, and Channel Estimation (CE). CE allows use of coherent modulation. Time and frequency correlation have been exploited efficiently [8, 9] via use of the discrete prolate spheroidal (DPS) sequences [10].

We combine the iterative receiver for MIMO-OFDM systems in [7] with the bidimensional estimator in [9], meant to operate in time-frequency variant environments, i.e. where the channel exhibits correlation in both time and frequency. The paper is organized as follows: the model for the MIMO-OFDM system is described in Sec. 2; in Sec. 3 we develop the iterative receiver; Sec. 4 shows the performance obtained via simulations; some concluding remarks are given in Sec. 5.

Notation - Column vectors (resp. matrices) are denoted with lower (resp. upper)-case bold letters; a_i (resp. $A_{i,j}$) denotes the ith (resp. (i,j)th) element of vector $\boldsymbol{a}$ (resp. matrix $\boldsymbol{A}$); $\mathrm{diag}(\boldsymbol{a})$ denotes a diagonal matrix whose main diagonal is $\boldsymbol{a}$. $\boldsymbol{I}_N$ denotes the $N \times N$ identity matrix; $\boldsymbol{i}_N^{(n)}$ denotes the nth column of $\boldsymbol{I}_N$; $\boldsymbol{e}_N$ (resp. $\boldsymbol{o}_N$) denotes a vector of length N whose elements are 1 (resp. 0); $\mathbb{E}\{.\}$, $(.)^*$, $(.)^{\mathrm{T}}$ and $(.)^{\mathrm{H}}$ denote expectation, conjugate, transpose and conjugate transpose operators; $\otimes$ is the Kronecker matrix product; $\Re(a)$ and $\Im(a)$ denote the real and imaginary parts of a; $\lceil a \rceil$ denotes the smallest integer value greater or equal than a; j is the imaginary unit; $\mathcal{N}(\mu, \sigma^2)$ is the normal distribution with mean μ and variance σ^2; $\mathcal{N}_{\mathbb{C}}(\boldsymbol{\mu}, \boldsymbol{\Sigma})$ is the circular symmetric complex normal distribution with mean vector $\boldsymbol{\mu}$ and covariance matrix $\boldsymbol{\Sigma}$; symbol $\sim$ means "distributed as".

2. SYSTEM MODEL

We consider a MIMO-OFDM system with K transmit antennas (TAs) and N receive antennas (RAs) and assume that each transmit antenna sends an independent data stream(e.g. a scenario with K different users with one single TA and one base station with N RAs). The transmission is frame oriented: the bit stream of each TA is divided in groups of L_b source bits; each group is encoded via a convolutional encoder and a random interleaver; L_p pilot bits are inserted to produce a frame of L code bits. Code bits are mapped into symbols via QPSK modulation, i.e. $L_x = L/2$ symbols per frame. The frame is divided into $S = L_x/M$ blocks, with M being the number of subcarriers. Each block provides an OFDM symbol to be transmitted on the wireless channel, thus each codeword spans both time and frequency dimensions.

We assume that pilot QPSK symbols are distributed in the frame according to a hexagonal grid in which M_p subcarriers present S_p pilots each, thus having $L_p/2 = M_p S_p$ pilots per frame, i.e. a pilot-to-symbol ratio (PSR) L_p/L. More specifically, we assume that the subcarriers in which pilots are present are given by the following set of indexes $\left\{\left\lceil \frac{(2m-1)M}{2M_p} \right\rceil\right\}_{m=1}^{M_p}$. Also, referring to the mth subcarrier among those containing pilots, pilots are distributed according to the following set of time indexes $\left\{\mathrm{mod}\left(\left\lceil \frac{(2s-1)S}{2S_p} \right\rceil + \left\lceil \frac{(m-1)S}{2S_p} \right\rceil, S\right)\right\}_{s=1}^{S_p}$.

In the following, $b_k[\ell]$ and $c_k[\ell]$ denote the ℓth source bit and the ℓth code bit (including pilots), to be transmitted by the kth TA. Also, referring to the mth subcarrier during transmission of the sth OFDM symbol: $x_k[m,s]$ denotes the symbol transmitted by the kth TA; $H_{n,k}[m,s]$ denotes the channel coefficient between the kth TA and the nth RA; $w_n[m,s]$

This work has been supported by the Research Council of Norway under the project WILATI within the NORDITE framework (grant 172239/S10).

denotes the additive noise at the nth RA; $r_n[m,s]$ denotes the received signal at the nth RA. QPSK mapping is based on $\boldsymbol{x}[m,s] = (c_k(2\ell-1) - jc_k(2\ell))/\sqrt{2}$, while demapping on $c_k(2\ell-1) = \Re(x_k[m,s])$ and $c_k(2\ell) = -\Im(x_k[m,s])$, where $\ell = (s-1)M + m$. Assume the length of the cyclic prefix exceeds the channel delay spread, and denote the transmitted vector, the noise vector ($\sim \mathcal{N}_{\mathbb{C}}(\boldsymbol{o}_N, \sigma_w^2 \boldsymbol{I}_N)$), the received vector, and the channel matrix

$$\begin{aligned} \boldsymbol{x}[m,s] &= (x_1[m,s], \ldots, x_K[m,s])^{\mathrm{T}} \\ \boldsymbol{w}[m,s] &= (w_1[m,s], \ldots, w_N[m,s])^{\mathrm{T}} \ , \\ \boldsymbol{r}[m,s] &= (r_1[m,s], \ldots, r_N[m,s])^{\mathrm{T}} \ , \end{aligned} \qquad \boldsymbol{H}[m,s] = \begin{pmatrix} H_{1,1}[m,s] & \ldots & H_{1,K}[m,s] \\ \vdots & \ddots & \vdots \\ H_{N,1}[m,s] & \ldots & H_{N,K}[m,s] \end{pmatrix} ,$$

then the discrete-time model for the received signal is

$$\boldsymbol{r}[m,s] = \boldsymbol{H}[m,s]\boldsymbol{x}[m,s] + \boldsymbol{w}[m,s] \ . \tag{1}$$

Also, we denote the channel vector from kth TA as $\boldsymbol{h}_{(k)}[m,s] = \boldsymbol{H}[m,s]\boldsymbol{i}_K^{(k)}$.

3. ITERATIVE RECEIVER

Transmissions from the various TAs combine at each RA and are jointly processed to unveil the original bitstreams. Each OFDM symbol is demodulated and sent to the iterative decoder, which performs three tasks: **(i) MUD** - via Parallel Interference Cancellation (PIC) and Minimum Mean Square Error (MMSE) filtering [2, 5, 6, 7]; *"input"*: received data from the demodulator, extrinsic code information from the Soft-Input Soft-Output (SISO) decoders, channel estimates from the channel estimator; *"output"*: extrinsic symbol information to the SISO decoders; **(ii) SISO Decoding** - via BCJR algorithm [11]; *"input"*: extrinsic symbol information from the MUD; *"output"*: extrinsic code information to the MUD, *a posteriori* code information to the channel estimator, *a posteriori* source information as final output; **(iii) CE** - via bidimensional Slepian expansion and Linear MMSE (LMMSE) estimation [9]; *"input"*: received data from the demodulator, *a posteriori* code information from the SISO decoders; *"output"*: channel estimates to the MUD.

Both the multi-user detector and the SISO decoders exchange extrinsic-based soft information on symbols x_k. We denote $\tilde{x_k}$ the one passing from the SISO decoders to the multi-user detector, and $\tilde{z_k}$ the one passing from the multi-user detector to the SISO decoders. SISO decoders also provide *a posteriori*-based soft information on symbol x_k, denoted $\hat{x_k}$, to the channel estimator. The channel estimator provides channel coefficient estimates, denoted $\hat{H}_{n,k}$.

It is worth noticing that SISO decoders pre-process $\{\tilde{z_k}[1], \ldots, \tilde{z_k}[L_x]\}$ via demapping and deinterleaving, and post-process $\{\tilde{x_k}[1], \ldots, \tilde{x_k}[L_x]\}$ and $\{\hat{x_k}[1], \ldots, \hat{x_k}[L_x]\}$ via interleaving and mapping.

3.1. MUD

The received signals (1) are processed separately for each subcarrier and for each OFDM symbol. We omit the indexes m and s to simplify notation. Also, we assume that the receiver has perfect knowledge of the channel coefficients, while in practice estimates from the channel estimator are used ($\boldsymbol{H}$ is replaced with $\hat{\boldsymbol{H}}$).

The PIC block receives $\tilde{\boldsymbol{x}}$ from the SISO decoders and $\boldsymbol{H}$ from the channel estimator. The interference component for the kth TA is $\boldsymbol{H}\tilde{\boldsymbol{x}}_{(k)}$, where $\tilde{\boldsymbol{x}}_{(k)} = \tilde{\boldsymbol{x}} - \tilde{x}_k \boldsymbol{i}_K^{(k)}$, then for each TA it is possible to compute the residual term from the interference cancellation as $\tilde{\boldsymbol{r}}_{(k)} = \boldsymbol{r} - \boldsymbol{H}\tilde{\boldsymbol{x}}_{(k)}$. The residual term is then processed with an MMSE filter, to reduce further the effects of noise and interference, giving the extrinsic-based soft information

$$\tilde{z}_k = \frac{\boldsymbol{i}_K^{(k)\mathrm{T}} \left(\boldsymbol{H}^{\mathrm{H}}\boldsymbol{H} + \sigma_w^2 \boldsymbol{V}_{(k)}^{-1}\right)^{-1} \boldsymbol{H}^{\mathrm{H}} \tilde{\boldsymbol{r}}_{(k)}}{\boldsymbol{i}_K^{(k)\mathrm{T}} \left(\boldsymbol{H}^{\mathrm{H}}\boldsymbol{H} + \sigma_w^2 \boldsymbol{V}_{(k)}^{-1}\right)^{-1} \boldsymbol{H}^{\mathrm{H}} \boldsymbol{h}_{(k)}} ,$$

where $\boldsymbol{V}_{(k)} = \mathrm{diag}\left((1-|\tilde{x}_1|^2, \ldots, 1-|\tilde{x}_{k-1}|^2, 1, 1-|\tilde{x}_{k+1}|^2, \ldots, 1-|\tilde{x}_K|^2)\right)$. For the derivation refer to [7].

3.2. SISO Decoding

After collecting $\{\tilde{z}_k[1], \ldots, \tilde{z}_k[L_x]\}$, each TA can be decoded independently using the BCJR algorithm [11]. The model for the output of the multi-user detector [2], used by the single SISO decoder for the kth TA, is $\tilde{z}_k = \mu_k x_k + v_k$, with $v_k \sim \mathcal{N}(0, \eta_k^2)$, where $\mu_k = 1$, and $\eta_k^2 = \left(\boldsymbol{i}_K^{(k)\mathrm{T}} \left(\boldsymbol{H}^{\mathrm{H}}\boldsymbol{H} + \sigma_w^2 \boldsymbol{V}_{(k)}^{-1}\right)^{-1} \boldsymbol{H}^{\mathrm{H}} \boldsymbol{h}_{(k)}\right)^{-1}$.

The algorithm has been implemented in the log-domain [12]. The initialization of forward and backward variables takes into account that the encoder starts and stops (due to the insertion of tail bits within each frame) in state 1.

3.3. CE

Assume a time-frequency variant channel with maximum normalized delay spread $\eta_{\max}^{(\mathrm{d})}$ and maximum normalized Doppler spread $\nu_{\max}^{(\mathrm{D})}$, i.e. the support of the scattering function $\mathcal{H}_{n,k}(\eta,\nu) = \sum_{m=1}^{M}\sum_{s=1}^{S} H_{n,k}[m,s]\mathrm{e}^{-j2\pi(\eta m+\nu s)}$. Variables η and ν represent time and frequency as they correspond via a Fourier transformation to frequency index m and time index s, and account for delay and Doppler, respectively. We consider the bidimensional Slepian expansion

$$H_{n,k}[m,s] \approx \sum_{\ell=1}^{L}\sum_{i=1}^{I} \psi_{n,k}[\ell,i]u_i[s]v_\ell[m] \;, \tag{2}$$

where $\psi_{n,k}[\ell,i]$ is the (ℓ,i)th Slepian coefficient for the link between the kth TA and the nth RA; $v_\ell[m]$ (resp. $u_i[s]$) is the mth (resp. sth) sample of the ℓth (resp. ith) DPS sequence for the frequency (resp. time) interval $\{1,\ldots,M\}$ (resp. $\{1,\ldots,S\}$) and delay (resp. Doppler) extension $\eta_{\max}^{(\mathrm{d})}$ (resp. $\nu_{\max}^{(\mathrm{D})}$). DPS sequences are defined as the solutions to $\sum_{m'=1}^{M} 2\eta_{\max}^{(\mathrm{d})}\mathrm{sinc}\left(2\eta_{\max}^{(\mathrm{d})}(m'-m)\right)v_\ell[m'] = \lambda_\ell^{(\mathrm{d})}v_\ell[m]$ $\left(\text{resp. } \sum_{s'=1}^{S} 2\nu_{\max}^{(\mathrm{D})}\mathrm{sinc}\left(2\nu_{\max}^{(\mathrm{D})}(s'-s)\right)u_i[s'] = \lambda_i^{(\mathrm{D})}u_i[s]\right)$, with $\lambda_\ell^{(\mathrm{d})}$ and $\lambda_i^{(\mathrm{D})}$ denoting the corresponding eigenvalues. In (2) the limits of the sums are $M^{(\mathrm{d})} \le L \le M$ and $S^{(\mathrm{D})} \le I \le S$, being $M^{(\mathrm{d})} = \left\lceil 2\eta_{\max}^{(\mathrm{d})}M\right\rceil + 1$ and $S^{(\mathrm{D})} = \left\lceil 2\nu_{\max}^{(\mathrm{D})}S\right\rceil + 1$ the approximate signal space extensions. Space concentration, is due to the eigenvalues $\lambda_\ell^{(\mathrm{d})}$ (resp. $\lambda_i^{(\mathrm{D})}$) becoming negligible for $\ell > 2\eta_{\max}^{(\mathrm{d})}S$ (resp. $i > 2\nu_{\max}^{(\mathrm{D})}S$).

Let $\boldsymbol{v}[m] = (v_1[m],\ldots,v_L[m])^{\mathrm{T}}$, $\boldsymbol{u}[s] = (u_1[s],\ldots,u_I[s])^{\mathrm{T}}$, $\boldsymbol{\lambda}^{(\mathrm{d})} = \left(\lambda_1^{(\mathrm{d})},\ldots,\lambda_L^{(\mathrm{d})}\right)^{\mathrm{T}}$, $\boldsymbol{\lambda}^{(\mathrm{D})} = \left(\lambda_1^{(\mathrm{D})},\ldots,\lambda_I^{(\mathrm{D})}\right)^{\mathrm{T}}$; and collect the received signals, $\boldsymbol{r}[s] = \left(\boldsymbol{r}^{\mathrm{T}}[1,s],\ldots,\boldsymbol{r}^{\mathrm{T}}[M,s]\right)^{\mathrm{T}}$, $\boldsymbol{r} = \left(\boldsymbol{r}^{\mathrm{T}}[1],\ldots,\boldsymbol{r}^{\mathrm{T}}[S]\right)^{\mathrm{T}}$; the transmitted signals, $\boldsymbol{\Xi}[m,s] = \boldsymbol{I}_N \otimes (\boldsymbol{x}[m,s]\otimes\boldsymbol{v}[m]\otimes\boldsymbol{u}[s])^{\mathrm{T}}$, $\boldsymbol{\Xi}[s] = \left(\boldsymbol{\Xi}^{\mathrm{T}}[1,s],\ldots,\boldsymbol{\Xi}^{\mathrm{T}}[M,s]\right)^{\mathrm{T}}$, $\boldsymbol{\Xi} = \left(\boldsymbol{\Xi}^{\mathrm{T}}[1],\ldots,\boldsymbol{\Xi}^{\mathrm{T}}[S]\right)^{\mathrm{T}}$; the Slepian coefficients, $\boldsymbol{\psi}_{n,k}[\ell] = (\psi_{n,k}[\ell,1],\ldots,\psi_{n,k}[\ell,I])^{\mathrm{T}}$, $\boldsymbol{\psi}_{n,k} = \left(\boldsymbol{\psi}_{n,k}^{\mathrm{T}}[1],\ldots,\boldsymbol{\psi}_{n,k}^{\mathrm{T}}[L]\right)^{\mathrm{T}}$, $\boldsymbol{\psi}_n = \left(\boldsymbol{\psi}_{n,1}^{\mathrm{T}},\ldots,\boldsymbol{\psi}_{n,K}^{\mathrm{T}}\right)^{\mathrm{T}}$, $\boldsymbol{\psi} = \left(\boldsymbol{\psi}_1^{\mathrm{T}},\ldots,\boldsymbol{\psi}_N^{\mathrm{T}}\right)^{\mathrm{T}}$; and the noise, $\boldsymbol{w} = \left(\boldsymbol{w}^{\mathrm{T}}[1],\ldots,\boldsymbol{w}^{\mathrm{T}}[S]\right)^{\mathrm{T}}$, $\boldsymbol{w}[s] = \left(\boldsymbol{w}^{\mathrm{T}}[1,s],\ldots,\boldsymbol{w}^{\mathrm{T}}[M,s]\right)^{\mathrm{T}}$; the signal model for CE is $\boldsymbol{r} = \boldsymbol{\Xi}\boldsymbol{\psi} + \boldsymbol{w}$, giving the following LMMSE channel estimate [9] to be used in (2)

$$\hat{\boldsymbol{\psi}} = \left(\hat{\boldsymbol{\Xi}}^{\mathrm{H}}\boldsymbol{\Delta}^{-1}\hat{\boldsymbol{\Xi}} + \boldsymbol{C}_\psi^{-1}\right)^{-1}\hat{\boldsymbol{\Xi}}^{\mathrm{H}}\boldsymbol{\Delta}^{-1}\boldsymbol{r} \;,$$

where $\boldsymbol{C}_\psi = \frac{1}{2\eta_{\max}^{(\mathrm{d})}}\frac{1}{2\nu_{\max}^{(\mathrm{D})}}\mathrm{diag}\left(\boldsymbol{e}_{NK}\otimes\boldsymbol{\lambda}^{(\mathrm{d})}\otimes\boldsymbol{\lambda}^{(\mathrm{D})}\right)$ is the covariance matrix of the Slepian coefficients; $\hat{\boldsymbol{\Xi}} = \mathbb{E}\{\boldsymbol{\Xi}\}$ contains the expected transmitted symbols computed via *a posteriori*-based soft information from the SISO decoders; $\boldsymbol{\Delta} = \boldsymbol{\Theta} + \sigma_w^2\boldsymbol{I}_{NMS}$, $\boldsymbol{\Theta} = \mathrm{diag}(\boldsymbol{\vartheta})$, $\boldsymbol{\vartheta} = \left(\boldsymbol{\vartheta}^{\mathrm{T}}[1],\ldots,\boldsymbol{\vartheta}^{\mathrm{T}}[S]\right)^{\mathrm{T}}$, $\boldsymbol{\vartheta}[s] = \left(\boldsymbol{\vartheta}^{\mathrm{T}}[1,s],\ldots,\boldsymbol{\vartheta}^{\mathrm{T}}[M,s]\right)^{\mathrm{T}}$, $\boldsymbol{\vartheta}[m,s] = \left(\sum_{k=1}^{K}\left(1-|\hat{x}_k[m,s]|^2\right)\right)\boldsymbol{e}_N$. CE is evaluated via Normalized Mean Square Error (NMSE)

$$\delta_H = \frac{\mathbb{E}\{|H_{n,k}[m,s]-\hat{H}_{n,k}[m,s]|^2\}}{\mathbb{E}\{|H_{n,k}[m,s]|^2\}} \;.$$

4. SIMULATION RESULTS

Bit-Error Rate (BER) performance vs Signal-to-Noise Ratio (SNR) have been obtained via numerical simulations and compared with the case in which Perfect Channel State Information (PCSI) is assumed at the receiver.

Results shown here refer to 2×2 systems with $M = 32$ subcarriers and $S = 128$ OFDM symbols per frame, thus $L = 8192$ code bits per frame. Iteration number is set to 7. Time-frequency variant wireless channels were simulated via Rayleigh fading according to Jakes'model [13]. Channel coefficients for each TA-RA pair were generated according to a model with 15 interfering paths, maximum normalized delay spread $\eta_{\max}^{(\mathrm{d})} = 0.05$, and maximum normalized Doppler spread $\nu_{\max}^{(\mathrm{D})} = 0.005$. Delay-Doppler space reduces from $(M,S) = (32,128)$ to $(M^{(\mathrm{d})},S^{(\mathrm{D})}) = (5,3)$, and $L\times I = 8\times 6 = 48$ coefficients were used for the Slepian expansion.

In each frame we considered 4 different pilot configurations: (i) PSR= 0.44% with $M_p = 6$ and $S_p = 3$; (ii) PSR= 0.88% with $M_p = 12$ and $S_p = 3$; (iii) PSR= 0.88% with $M_p = 6$ and $S_p = 6$; (iv) PSR= 1.76% with $M_p = 12$ and $S_p = 6$; Excluding pilots we have respectively 8156, 8120, 8120, and 8048 code bits generated at rate $R = 1/2$ via a recursive systematic convolutional encoder with generators $(7,5)_8$ and with two tail bits used to enforce the final state into 1, thus $L_b = 4076$, $L_b = 4058$, $L_b = 4058$, and $L_b = 4022$ source bits per frame, respectively.

Fig. 1 shows the performance of the different pilot configurations compared with the PCSI case. From the sampling theorem point of view, configuration (i) should be sufficient to estimate the channel, as pilot spacing doubles Nyquist rate. However it is apparent from the simulations that twice Nyquist rate is not sufficient for the turbo effect to lead the system

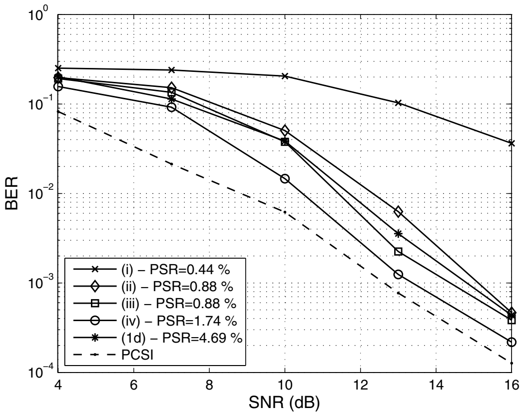

Fig. 1. BER-vs-SNR for a 2×2 system.

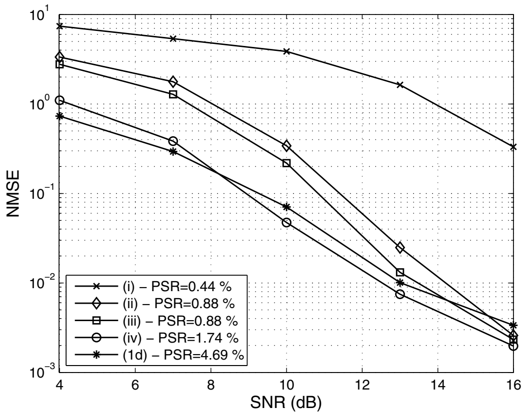

Fig. 2. NMSE-vs-SNR for a 2×2 system.

approach the PCSI case. Oversampling is necessary: configurations (ii) and (iii) double the sampling rate in frequency and time, respectively, with consequent improvement. Finally configuration (iv), oversampling in both dimensions, gave excellent performance. As comparison, Fig. 1 also shows the performance of the system in [7]. Denoted as (1d), it uses a monodimensional channel estimator, with pilots on all the subcarriers ($M_p = M$, $S_p = 6$), i.e. PSR= 4.69%.

It is worth noticing that the number of pilots in the case (1d) is slightly less than 3 times the number of pilots in the case (iv) although the latter experience much better performance. The reason lies in the use of the bidimensional channel estimation. The counter effect is an increased computational complexity. Fig. 2 shows the corresponding performance of the channel estimator that follows the same trend of the whole system.

5. CONCLUSION

An iterative receiver performing joint MUD, SISO decoding and CE for MIMO-OFDM systems in time-frequency variant wireless channels has been presented. It implements PIC and MMSE filtering for MUD, bidimensional Slepian expansion and LMMSE estimation for CE, log-domain BCJR algorithm for single-user SISO decoding. Simulations with convolutional coding and QPSK modulation showed excellent performance in terms of BER-vs-SNR. Small amount of pilots is needed to approach the PCSI case with vanishing degradation.

6. REFERENCES

[1] G.L. Stüber, J.R. Barry, S.W. McLaughlin, Y. Li, M.A. Ingram, T.G. Pratt, "Broadband MIMO-OFDM Wireless Communications," *Proc. IEEE*, vol. 92, no. 2, pp. 271–294, February 2004.

[2] X. Wang, H.V. Poor, "Iterative (Turbo) Soft Interference Cancellation and Decoding for Coded CDMA," *IEEE Trans. Commun.*, vol. 47, no. 7, pp. 1046–1061, July 1999.

[3] J. Boutros, G. Caire, "Iterative Multiuser Joint Decoding: Unified Framework and Asymptotic Analysis," *IEEE Trans. Inf. Theory*, vol. 48, no. 7, pp. 1772–1793, July 2002.

[4] G. Caire, R.R. Müller, T. Tanaka, "Iterative Multiuser Joint Decoding: Optimal Power Allocation and Low-Complexity Implementation," *IEEE Trans. Inf. Theory*, vol. 50, no. 9, pp. 1950–1973, September 2004.

[5] M. Lončar, R.R. Müller, J. Wehinger, C.F. Mecklenbräuer, T. Abe, "Iterative Channel Estimation and Data Detection in Frequency-Selective Fading MIMO Channels," *European Trans. Telecommun.*, vol. 15, no. 5, pp. 459–470, October 2004.

[6] T. Zemen, C.F. Mecklenbräuker, J. Wehinger, R.R. Müller, "Iterative Joint Time-Variant Channel Estimation and Multi-User Detection for MC-CDMA," *IEEE Trans. Wireless Commun.*, vol. 5, no. 6, pp. 1469–1478, June 2006.

[7] P. Salvo Rossi, R.R. Müller, "Joint Iterative Time-Variant Channel Estimation and Multi-User Detection for MIMO-OFDM Systems," *IEEE Global Temecommun. Conf. (GLOBECOM)*, pp. 4263–4268, November 2007.

[8] T. Zemen, C.F. Mecklenbräuker, "Time-Variant Channel Estimation Using Discrete Prolate Spheroidal Sequences," *IEEE Trans. Signal Process.*, vol. 53, no. 9, pp. 3597–3607, September 2005.

[9] P. Salvo Rossi, R.R. Müller, "Slepian-Based 2-Dimensional Estimation of Time-Frequency Variant MIMO-OFDM Channels," *IEEE Signal Process. Lett.*, vol. 15, pp. 21-24, January 2002.

[10] D. Slepian, "Prolate Spheroidal Wave Functions, Fourier Analysis, and Uncertainty - V: The Discrete Case," *Bell Syst. Tech. J.*, vol. 57, no. 5, pp. 1371-1430, June 1978.

[11] L.R. Bahl, J. Cocke, F. Jelinek, J. Raviv, "Optimal Decoding of Linear Codes for Minimizing Symbol Error Rate," *IEEE Trans. Inf. Theory*, vol. 20, no. 2, pp. 284–287, March 1974.

[12] P. Robertson, E. Villebrun, E. Höher, "A Comparison of Optimal and Sub-Optimal MAP Decoding Algorithms Operating in the Log Domain," *IEEE Int. Conf. Commun. (ICC)*, vol. 2, pp. 1009–1013, June 1995.

[13] Y.R. Zheng, C. Xiao, "Simulation Models with Correct Statistical Properties for Rayleigh Fading Channels," *IEEE Trans. Commun.*, vol. 51, no. 6, pp. 920–928, June 2003.